약학석사학위논문

Comparison of metabolite profiles of normal and cancer cell lines in response to cytotoxic agents

Cytotoxic agents 를 처리하였을 때

정상세포와 암세포에서 metabolic profile 의 비교

2014년 8월

서울대학교 대학원

약학과 천연물과학전공

이 수 진

Comparison of metabolite profiles of normal and cancer cell lines in response to cytotoxic agents

Cytotoxic agents를 처리하였을 때
정상세포와 암세포에서 metabolic profile의 비교

지도교수 박 성 혁
이 논문을 약학석사학위논문으로 제출함

2014년 7월

서울대학교 대학원
약학과 천연물과학전공
이 수 진

이 수 진의 석사학위논문을 인준함
2014년 7월

위 원 장 _____ (인)

부위원장 _____ (인)

위 원 _____ (인)

Abstract

Comparison of metabolite profiles of normal and cancer cell lines in response to cytotoxic agents

LEE SU JIN

Natural Products Science Major

College of Pharmacy

The Graduate School

Seoul National University

Together with radiotherapy, chemotherapy using cytotoxic agents is one of the most common therapies in cancer. Metabolic changes in cancer cells are drawing much attention recently, but the metabolic alterations by anticancer agents have not been much studied. Here, we investigated the effects of commonly used cytotoxic agents on lung normal cell MRC5 and lung cancer cell A549. We employed Cis-

plastin, Doxorubicin, and 5-Fluorouracil (5-FU) and compared their effects on the viability and metabolism of the normal and cancer cell lines. We first established the concentration of the cytotoxic reagents that give differences in the viabilities of normal and cancer cell lines. In those conditions, the viability of A549 decreased significantly (p-value = 0.001), whereas that of MRC5 remained unchanged (p-value = 0.358). To study the metabolic alterations implicated in the viability differences, we obtained the metabolic profiles using 1H-NMR spectrometry. The 1H-NMR data showed that the metabolic changes of A549 cells are more remarkable than that of MRC5 cells and the effect of 5-FU on the A549 cells is the most distinct compared to other treatments. Heat map analysis showed that metabolic alterations under treatment of cytotoxic agents are totally different between normal and cancer cells. Multivariate analysis and weighted correlation network analysis (WGCNA) revealed a distinctive metabolite signature and hub metabolites. Two different analysis tools revealed that the changes of cell metabolism in response to cytotoxic agents were highly correlated with the Warburg effect and Reductive lipogenesis, two pathways having important effects on the cell survival. Taken together, our study addressed the correlation between the viability and metabolic profiles of MRC5 and A549 cells upon the treatment of cytotoxic anticancer agents.

Keywords: Lung cancer cell, Chemotherapy, Cytotoxic agents, Metabolic profile, NMR spectroscopy

Student number: 2012-23595

Contents

List of Tables

List of Figures

Ⅰ. Introduction

Cytotoxic agents play an important role in cancer therapy due to their efficacies, and attract much attention from researchers (1). Among cytotoxic agents, Cis-platin, Doxorubicin, and 5-FU have been used for decades, and are still widely applied in treatment of different types of cancer and especially in lung cancer. While Cis-platin and Doxorubicin inflict damage on DNA directly, 5-FU, a thymidylate synthase inhibitor blocks the synthesis of thymidine during the DNA replication (2-4). The targets of most cytotoxic agents are well established, but cellular metabolic alterations during the cytotoxic action have not been clearly understood yet (5).

Cellular metabolism in cancer is becoming more important, since oncogenic signaling pathways have been demonstrated to connect with the metabolic activities and strategies for curing cancer can be gained from simple metabolic alterations (6). The changes of single amino acids are in the context also focused, as their effect on metabolism cannot be overlooked, and representative amino acids are followings: glycine, serine, glutamine, and glucose (7-10).

It is known that the metabolic characteristics of cancer cells are distinct from those of normal cells. In cancer cells, energy is generated by the aerobic glycolysis process rather than the mitochondria oxidative phosphorylation process (11, 12). Aerobic glycolysis of cancer cell proceeds in normoxic conditions, which is

distinguished from the anaerobic glycolysis of normal cell. According to such phenomenon called “Warburg effect”, cancer cells uptake glucose rapidly, generate the adenosine 5-triphosphate (ATP) by inefficient way, and produce lots of lactates that made the extracellular environment acidic (6). In acidic condition cancer cells can easily metastasize to distant tissues. In addition to glycolysis, glutamiolysis, which starts from glutamine decomposition by glutaminase (GLS) and provides its products to tricarboxylic acid (TCA) cycle also increases in cancer cells (13). Multiple studies revealed that increased glutaminolysis is related to MYC transcription factor and it makes glutamine uptake and catabolism increase (14, 15). Glutaminolysis also has been receiving attention due to “Reductive lipogenesis”. This lipid synthesis pathway uses TCA intermediates derived from glutaminolysis as a source. Glutamine-derived α-ketoglutarate is reduced to citrate in mitochondria or cytosol by isocitrate dehydrogenase 1 (IDH1) or isocitrate dehydrogenase2 (IDH2), and converted to acetyl-CoA for lipid synthesis (6). Since rapidly dividing cancer cells requires more lipid as plasma membrane components apart from DNA, lipid synthesis is more important in cancer cells (16). Therefore, the point that cancer cell needs lots of lipid and mainly uses different pathway from normal cell for the lipid synthesis is the unique feature of cancer cells. Finally, the Pentose phosphate pathway (PPP) also contributes the cancer specific metabolic alterations. PPP specifically increases in cancer cells. Glucose-6-phosphate (G6P), an intermediate of glycolysis is converted to ribulose-5-p by PPP producing the NADPH and GSH which can be provided for reducing the level of ROS. ROS level

alters the metabolic activities of cancer cells, and possibly causes cancer cell growth limitation or cancer cell death, so ROS level is an important issue on cancer metabolism (17). Understanding the features in cancer metabolism could provide strategies to exploit the cancer metabolism for the cancer treatment. Moreover, studies, how metabolisms are differently changed in normal and cancer cell lines in response to cytotoxic agents, could give more information available during chemotherapy in the clinical practice.

Metabolomics has been proven to be a pivotal tool in cancer metabolism research (18). This approach captures the cellular changes at the post translation level and identifies the biomarkers for evaluating the therapeutic effect and toxicity (19, 20). Commonly, NMR and Mass Spectrometry are widely employed in metabolomics study. To analyze the data obtained from spectrometry, various analasis or statistical tools are being used. In this study, using 1H-NMR based metabolomics, we characterized metabolic profiles of lung cancer cell A549 and normal lung cell MRC5 treated with three different cytotoxic agents: Cis-platin, Doxorubicin, and 5-FU. We could separate the three cytotoxic agent-treated groups in both normal and cancer cells, and identify biomarkers for each treatment group.

Ⅱ. Materials and Methods

1. Cell Culture

The human lung carcinoma cell line A549 was purchased from Korean Cell Line Bank (KCBL, Seoul, Korea) and cultured in 100π tissue culture dishes (BD Falcon, Bedford, MA, USA) containing Dulbecco's Modified Eagle's Medium (DMEM, Welgene, Daegu, Korea). The human lung fibroblast cell line MRC5 was purchased from American Type Culture Collection (ATCC CCL-171™, Manassas, VA, USA) and culture in 100π tissue culture dishes (BD Falcon, Bedford, MA, USA) containing Dulbecco's Modified Eagle's Medium (DMEM, Welgene, Daegu, Korea). Both media were supplemented with 10% fetal bovine serum (FBS, Welgene, Daegu, Korea), penicillin (100 U/ml, Welgene, Daegu, Korea) and streptomycin (100 ug/ml), and maintained at 37 ℃ in a humidified incubator under 5% CO2.

2. Cell Treatment

A549 and MRC5 cells were cultured in DMEM, washed with Dulbecco's Phosphate Buffered Saline (DPBS, Welgene, Deagu, Korea), detached with Trypsin/EDTA (Welgene, Daegu, Korea) and harvested harvested to 15 ml conical tube by centrifugation. Cells were plated in 96-well tissue culture plates (BD

Falcon, Bedford, MA, USA) at a cell density of 1.0 x 10^4 cells/well for MTT cell viability assay and cultured in 37 ℃ incubator under 5% CO2 to allow them to reattach. Cells were plated in 100π tissue culture dish (BD Falcon, Bedford, MA, USA) at a cell density of 0.8 x 10^6 cells/well for NMR spectroscopy and cultured in 37 ℃ incubator under 5% CO2 to allow them to reattach. After 4 h incubation, the culture media were supplemented with cytotoxic agents such as Cis-platin, Doxorubicin, and 5-FU (Sigma-Aldrich, St. Louis, MO, USA) at half maximal inhibitory concentration (IC50) and no cytotoxic agents were added in culture media of control cells. The used concentrations were 0.813 mg/ml, 0.13 mg/ml, and 0.0332 mg/ml for Cis-platin, Doxorubicin, and 5-FU respectively. The cells were incubated in 37 ℃ incubator under 5% CO2 for 72 h.

3. MTT Cell Viability Assay

Cell viability was evaluated by measuring the capacity of reducing the 3-(4,5-dimethylthiazol-2-yl)-2,5-diphenyltetrazolium bromide (MTT, Sigma-Aldrich, St. Louis, MO, USA) to formazan (21). In brief, MTT was dissolved in PBS at 5 mg/ml and MTT solution was added to each well. The 96-well plates were incubated at 37 ℃ for 4 h and then, the media was removed and 100 μl Dimethyl sulfoxide (DMSO, Sigma-Aldrich, St. Louis, MO, USA) was added into each well. After mixing thoroughly to dissolve the formazan in DMSO, the reducing capacity was measured by ELISA reader (Molecular Devices, Sunnyvale, CA, USA) at a

595 nm wavelength.

4. Sample Preparation for NMR Spectroscopy

Metabolites extraction was performed on both cell lines treated or untreated with each cytotoxic agent. A sample was equally counted with 0.8 X 10^6 cells. The metabolites of samples were extracted with the mixture of 100 μl methanol, 60 μl acetonitrile and 40 μl distilled water (22). The samples ware centrifuged at 21,000 g for 20 min at 4 ℃. The supernatants were collected and dried with speedvac (Vision Scientific, Bucheon, Korea). The samples were dissolved with a buffer composed of D2O, 2 mM Na2HPO4 and 5 mM NaH2PO4 containing a final concentration of 0.025% sodium-3-trimethyl silylpropionate (TSP, Cambridge Isotope Lab, Inc., Tewksbury, MA, USA) as an internal standard, which were transferred to 5 mm NMR tube.

5. NMR Measurements

One-dimensional NMR spectra were measured on a 500 MHz spectrometer (Bruker Biospin, Avance 500, Billerica, MA, USA) equipped with a cryogenic triple resonance probe. The acquisition parameters were essentially the same as those previously reported (23, 24). The metabolites were identified using Chenomx NMR software suite (Chenomx Inc., Edmonton, Alberta, Canada) by fitting the experimental spectra to those in the database and comparison with standard

compounds.

6. Multivariate Data Analysis

The time domain NMR data were Fourier transformed, phase corrected, and baseline corrected manually using MestReNova (Mestrelab Research, Santiago de Compostela, Spain). The processed NMR data were exported to an ASCII file and binned at a 0.003 ppm interval to reduce the complexity of the NMR data for pattern recognition. Moreover, the signals were normalized against total integration values and 0.025% TSP. The region corresponding to water (4.6–5.2 ppm) was removed from the spectra. The binning and normalization were performed using Perl software written in-house. The results were then imported into SIMCA-P version 11.0 (Umetrics, Umeå, Sweden). partial least squares-discrimination analysis (PLS-DA) and orthogonal projections to latent structure-discriminant analysis (OPLS-DA) were used for data analysis (25, 26). The p(corr) value was used to generate Heat map in Excel program with the highest value as red color and the lowest value as green color.

7. WGCNA Analysis

Spectral binning data were employed to perform weighted correlation network analysis (WGCNA) by following the standard procedure in reference (27, 28). The correlation network was constructed by calculating weighted Pearson correlation,

then using topological overlap to identify the similarity of bin values and grouping of highly similar correlation relationship into modules. The correlation between modules and traits (cytotoxic agents) was measured and only modules having $r>0.05$ and p-value < 0.05 were extracted for further investigation. In these modules, the bin values with the high connectivity with the others (≥ 5) were identified as hub values, which were then assigned for metabolites by Chenomx software.

Ⅲ. Results

1. Cell Viability by MTT Assay

For studying the action of cytotoxic agents on cell metabolism, the concentration of agents is important consideration. After 3 – day treatment of cytotoxic agents: Cis-platin, Doxorubicin, and 5-Fluorouracil (5-FU), we measured the cell viability of MRC5 and A549 cells by MTT assay, and ultimately gained the adequate concentrations of cytotoxic agents. We chose Cis-platin, doxorubicin and 5-FU concentration of 0.00813mg/10ml, 0.03319mg/10ml, and 0.00139mg/10ml respectively, corresponding to the half maximal inhibitory concentration (IC50). P value was calculated by an independent student's t-test. MTT assay data show the mean viability of each different treated group compared to control group (Figure 1.). The cell viabilities of all the treated groups decreased slightly after treating cytotoxic agents. However, the number of living cells is enough to look into the cellular metabolism. Under treatment with cytotoxic agents, the viability of A549 cancer cell decreased significantly compared to non-treated A549 cell group (p-value = 0.001), whereas that of MRC5 normal cell remained unchanged compared to non-treated MRC5 cell group (p-value = 0.358), so the concentrations of these agents were considered to be suitable to compare the metabolic profiles. Discrete p-value of each agent in A549 cell is 0.006, 0.010, and 0.000 for Cis-platin,

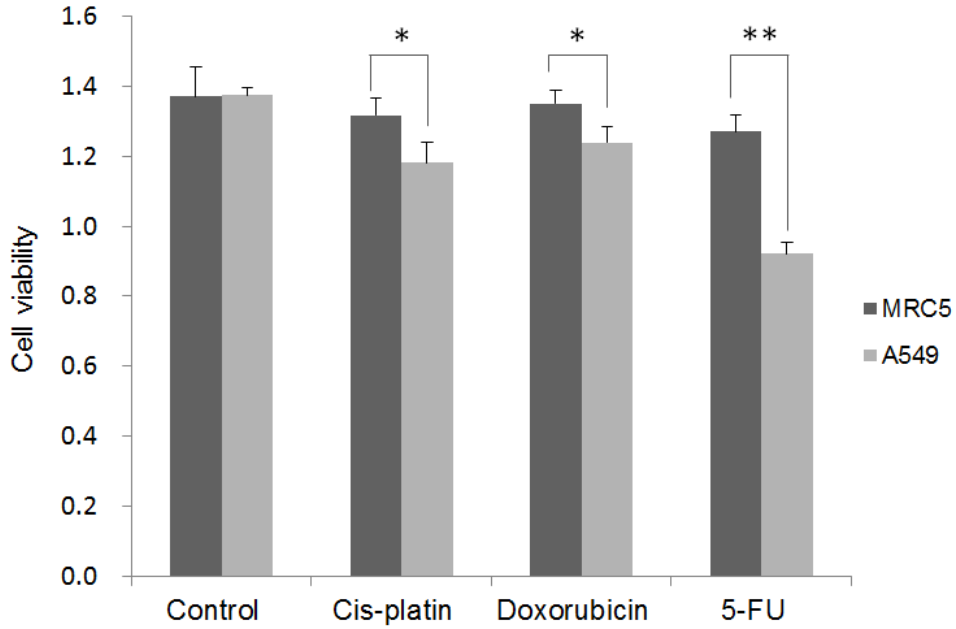

Figure 1. MTT Cell Viability Assay

After 3-day treatment of cytotoxic agents with the same concentration used in 1H-NMR spectroscopy, the viability of MRC5 and A549 cells was analyzed by MTT assay. Results show the mean viability of each different treatment group compared to control group. The viability in cytotoxic agent-treated A549 groups decreases significantly (p-value=0.001) whereas in the cytotoxic agent–treated MRC5 groups, the change in the viability is not significant (p-value=0.358)

*:p-value<0.05, **: p-value<0.01

Doxorubicin, and 5-FU respectively and that in MRC5 is 0.393, 0.727, and 0.150 for Cis-platin, Doxorubicin, and 5-FU respectively. Comparing the cell viability of A549 cells with that of MRC5 cells under each cytotoxic agent, there was a significant difference between A540 and MRC5 cell groups having the same treated agent (*:p-value<0.05, **:p-value<0.01). P-value was 0.041, 0.033, and 0.001 for Cis-platin, Doxorubicin, and 5-FU respectively. As shown here, the viability difference between A549 and MRC5 cells treated with 5-FU was the most significant. This result suggested that cytotoxic agents induced cell death have more impact on A549 cells than MRC5 cells, especially when treated with 5-FU.

2. NMR Spectral Data

DNA-damaging agents had an inhibition effect on the A549 cells and not a harmful effect on the MRC5 cells, so to find the metabolic differences related to such viability differences, we took a metabolic approach by 1H-NMR spectroscopy. The cytotoxic agents of Cis-platin, doxorubicin, and 5-FU were treated for 3 days with the same concentrations using in MTT cell viability assay. NMR data of MRC5 (A) and A549 (B) cells showed that the peak intensities were changed after treating the agents compared to the lowest control group in the four stacked NMR spectra (Figure 2.). The peaks of A549 cell were more changed in response to cytotoxic agents compared to that of MRC5 cell. In NMR spectra, the changes in the ranges of 3.5-4.5 ppm and 1.5-2.5 ppm were more noticeable in the A549 cells

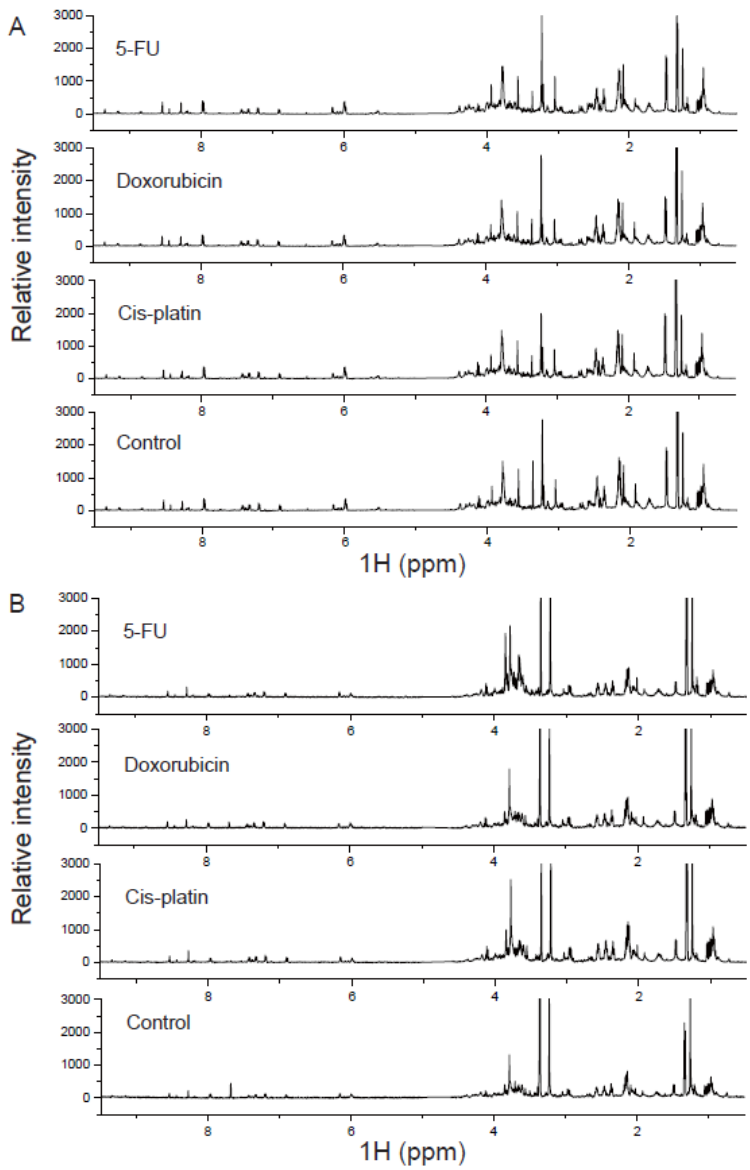

Figure 2. NMR Spectroscopy

1H-NMR spectra of MRC5 (A) and A549 (B) cells. NMR spectra were acquired after 3-day treatment with cytotoxic agents: Cis-platin, Doxorubicin, and 5-FU on 500MHz NMR spectrometer. The used concentration of Cis-platin, Doxorubicin, and 5-FU were mg/ml, 0.13 mg/ml, and 0.0332 mg/ml respectively.

than those in the MRC5 cells when treated with different cytotoxic agents. Especially, 5-FU treated A549 cells recorded the most distinctive spectra compared to other groups, which was consistent with MTT cell viability data in Figure 1. This result suggested that the cytotoxic agents affect the metabolic profile as well as DNA, and the effect is much greater on the A549 cell than the MRC5 cell, as seen in cell viability.

3. Multivariate Data Analysis

Multivariate analysis was applied to the NMR spectra to identify the general metabolic alterations and find the specific signals for the separation. Orthogonal projections to latent structure-discriminant analysis (OPLS-DA) score plots were made for MRC5 cells treated with Cis-platin (A) (R^2 = 0.987 and Q^2 = 0.771), Doxorubicin (C) (R^2 = 0.964 and Q^2 = 0.681), and 5-FU (E) (R^2 = 0.989 and Q^2 = 0.933) and A549 cells treated with Cis-platin (B) (R^2 = 0.986 and Q^2 = 0.865), Doxorubicin (D) (R^2 = 0.964 and Q^2 = 0.677), and 5-FU (F) (R^2 = 0.996 and Q^2 = 0.944) (Figure 3.). Each cytotoxic agent-treated groups were well separated from control in both MRC5 and A549 cells. We further used the partial least square-discriminant analysis (PLS-DA) score scatter plots to screen the differences among control and treated groups (Figure 4.). Control(black box), Cis-platin(red dot), Doxorubicin(green diamond) and 5-FU(blue triangle) groups were separated in both MRC5 (A) (R^2 = 0.980 and Q^2 = 0.779) and A549 (B) (R^2 = 0.988 and Q^2 =

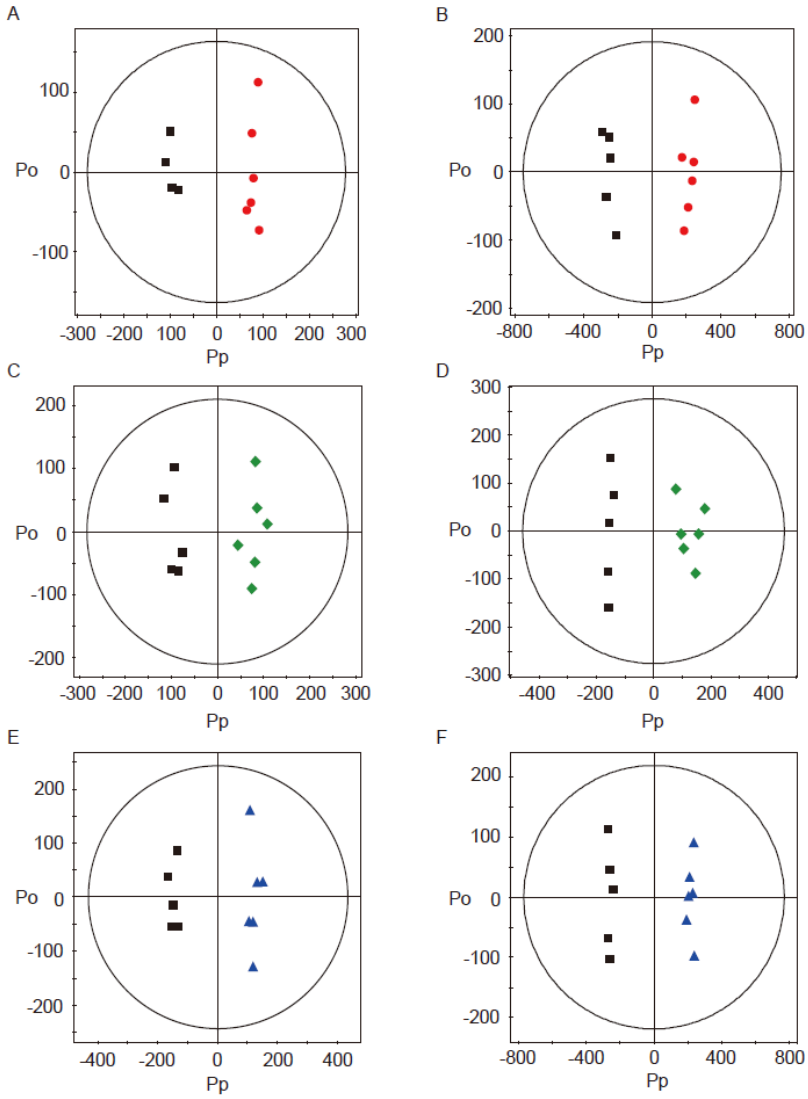

Figure 3. OPLS-DA Multivariate Analysis

Orthogonal projections to latent structure-discriminant analysis (OPLS-DA) score plots of MRC5 and A549 cells. MRC5 cells treated with Cis-platin (A), Doxorubicin (C), and 5-FU (E). A549 cells treated with Cis-platin (B), Doxorubicin (D), and 5-FU (F). Control(black box), Cis-platin(red dot), Doxorubicin(green diamond) and 5-FU(blue triangle) groups in both MRC5 and A549 cells.

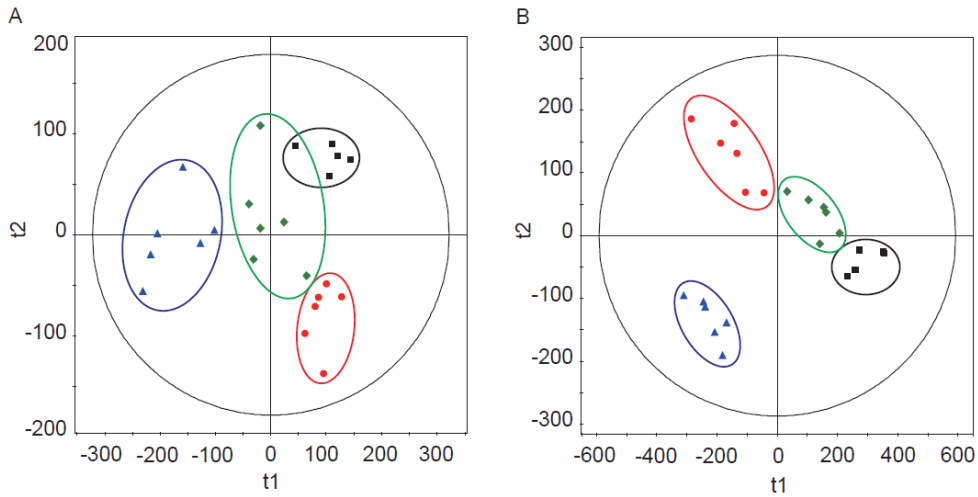

Figure 4. PLS-DA Multivariate Analysis

Partial least square-discriminant analysis (PLS-DA) plots of MRC5 (A) (R^2 = 0.980 and Q^2 = 0.779) and A549 (B) (R^2 = 0.988 and Q^2 = 0.876) cells treated with different cytotoxic agents. Control(black box), Cis-platin(red dot), Doxorubicin(green diamond) and 5-FU(blue triangle) groups in both MRC5 and A549 cells.

0.876) cells, only doxorubicin treated group of MRC5 cells slightly overlapped with the control group. 5-FU treated A549 cell group was particularly separated compared to other groups, suitable to the MTT viability result decreasing in 5-FU A549 cell group. PLS-DA data showed that cytotoxic agents caused the metabolic profiles of both MRC5 and A549 cells changed and the effect was the most in 5-FU treated A549 cells.

As shown in PLS-DA data, metabolic profiles in MRC5 normal cells and A549 cancer cells were both affected by cytotoxic agents, but we have known that there were differences in cell viabilities between MRC5 and A549 cells in response to cytotoxic agents from the result of MTT assay. In order to search for the candidate metabolites attributed to the cell viabilities, we assigned the each metabolites and conducted additional statistical analysis. Total of 25 metabolites were identified by Chenomax NMR software, and significant increase and decrease of each metabolite was determined by student's t-test with p-value<0.05 (Table 1). Metabolites of A549 cells were increased generally after treating each cytotoxic agent, whereas that of MRC5 cells were increased or decreased in different ways with A549 cells. Quantitative changes of metabolites after treating cytotoxic agents were different between MRC5 cells and A549 cells, and in many cases, these changes were made in opposite direction. Branched amino acids such as isoleucine, leucine and valine were significantly changed in all groups, further in opposite directions between MRC5 and A549 cells, and glucose, glutamine, and glutamate also showed the different changes between MRC5 and A549 cells.

Table 1. Assigned Metabolites

		Chemical shift & J-coupling (ppm and J values)	MRC5			A549		
			Cis /Con	Doxo /Con	5-FU /Con	Cis /Con	Doxo /Con	5-FU /Con
1	Alanine	1.48(d), 3.97(q)	-	▽	▽	▲	▲	-
2	Glycine	3.56(s)	-	-	-	▲	-	▲
3	Isoleucine	0.94(t), 1.02 (d)	▽	▽	▽	▲	▲	▲
4	Leucine	0.97(t), 1.72(m)	▽	▽	▽	▲	▲	▲
5	Valine	1.00(d), 1.05(d)	▽	▽	▽	▲	▲	▲
6	Glucose	3.83(m), 3.47(m), 3.24(t)	▲	▲	▲	-	-	-
7	Lactate	1.32(d), 4.11(q)	-	▽	▽	▲	▲	▲
8	Glutamine	2.15(m), 2.46(m), 3.78(t)	-	-	▽	▲	-	▲
9	Glutamate	2.04(m), 2.15(m), 2.36(m)	▽	-	-	▲	▲	▲
10	Glutathione	2.17(m), 2.56(m), 2.96(m), 3.81(m)	▽	-	▽	▲	▲	▲
11	Taurine	3.15(m), 3.28(m)	▽	▽	▽	▲	▲	-
12	Tyramine	6.90(d), 7.20(d)	▽	▽	▽	▲	-	-

13	Citrate	2.57(d), 2.68(s)	▲	-	-	▲	-	-
14	Phenylalanine	7.33(d), 7.38(t), 7.43(t)	▽	▽	▽	▲	▲	▲
15	Acetate	1.92(s)	▽	▽	▽	-	▲	-
16	Creatine	3.04(s), 3.93(s)	-	▽	▲	▲	▲	▲
17	Carnitine	3.21(s), 3.49(m)	▲	▲	▲	-	-	▲
18	Aspartate	2.67(q), 2.82(m)	▲	▲	▲	-	-	-
19	Allantoin	5.42(s)	-	-	-	-	-	-
20	Malonate	3.23(s)	▽	-	-	▲	-	▲
21	Xanthine	7.96(s)	-	-	-	-	-	▽
22	5,6-Dihydrouracil	2.55(t), 3.42(t)	▲	▲	▲	▲	-	▲
23	Trimethylamine N-oxide	3.36(s)	▽	▽	▽	▽	▽	▽
24	NAD+	6.05(d), 6.09(d), 8.20(t), 8.44(s), 8.84(d), 9.16(d), 9.34(s)	▲	-	▲	-	-	-
25	ANP	6.16(d), 8.27(s), 8.54(s)	-	-	▲	▲	-	▲

4. Heat Map Analysis

We used the het map analysis to illustrate the changes of metabolites systemically in both MRC5 and A549 cells in response to the cytotoxic agents (Figure 5.). The p(corr) was calculated for the each value to generate Heat map in Excel program with the highest value as red color and the lowest value as green color. The red color means that the corresponding metabolite was increased after treating cytotoxic agent, and the green color means that the corresponding metabolite was decreased after treating cytotoxic agent. We obtained the value divided by each control value in order to remove the cellular metabolic attributes that appear on their own, in other words, to separate the effects of cytotoxic agents, not from the cells in themselves. Heat map showed that there were distinct differences of metabolic alterations between MRC5 and A549 after treating cytotoxic agents, and the changing trend in response to cytotoxic agents were similar within three treatment groups in MRC5 cells, but less in A549 cells. Most of metabolites in A549 cells were shown in red color, whereas metabolites in MRC5 cells were more in green color, partially shown in red color. Looking at each metabolite, first, metabolites regarding to Warburg effect such as glucose and lactate were changed a lot in a reverse direction between MRC5 and A549 cells. Glucose was increased in MRC5 cells in response to cytotoxic agents in three treatment groups, but not changed in A549 cells, except 5-FU treated A549 group where glucose was slightly increased. Lactate was decreased in MRC5 cells, but increased in A549 cells. Second, glutamine regarding to reductive lipogenesis was

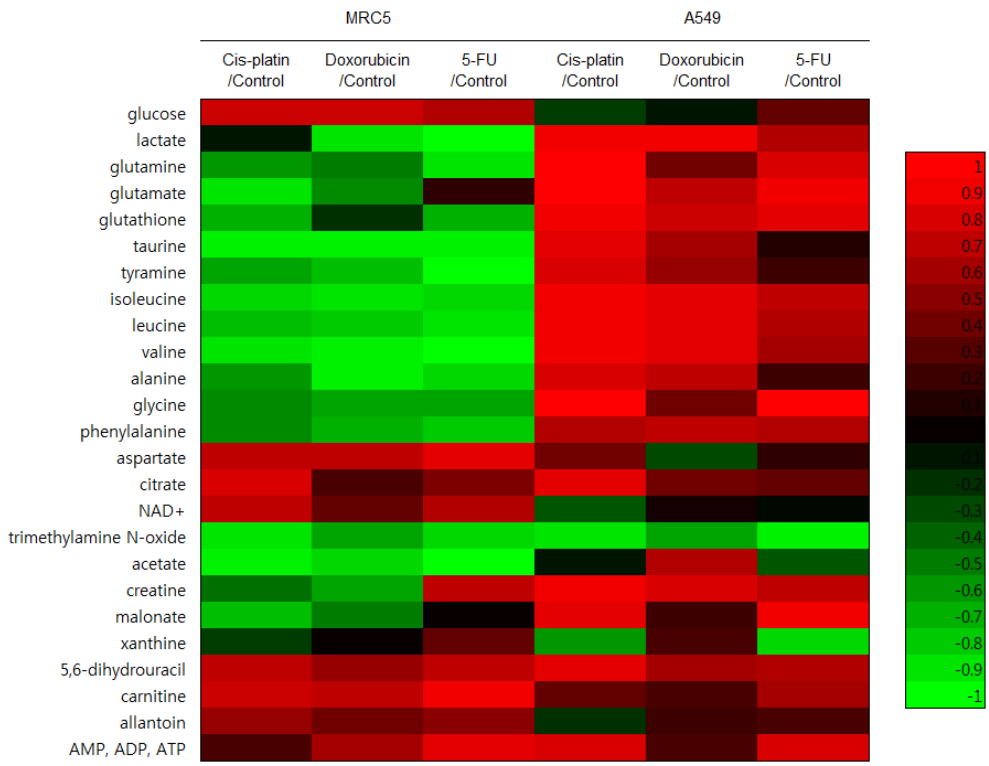

Figure 5. Heat Map Analysis

Heat map represents the metabolic changes in MRC5 and A549 cell treated with different cytotoxic agents. The p(corr) value was calculated for the each value to generate Heat map in Excel program with the highest value as red color and the lowest value as green color.

changed significantly as decreased in MRC5 cells, but increased in A549 cells in opposite direction. Third, glutathione and taurine related to Redox state were changed in opposite direction, as decreased in MRC5 cells and increased in A549 cells. Only taurine in 5-FU treated A549 cells was not increased. Fourth, branched amino acids such as isoleucine, leucine, and valine were changed significantly also in opposite direction. A total of branched amino acids was decreased in all groups of MRC5 cells and increased in all groups of A549 cells. Last, glycine was decreased in MRC5 cell groups and increased in A549 cell groups. Heat map result showed that same agent could differently effect on the each cell metabolism depending on cellular metabolic states.

5. Weighted Correlation Network Analysis

To confirm and complement the multivariate data, we used the methodologically different WGCNA analysis tool. Multivariate analysis shows the metabolic change or correlation in the level of individual metabolite, but WGCNA considers the metabolic network, in other words how they relate to each other. Applying the WGCNA into our NMR data, we identified the modules that are co-expressed metabolites groups, and visualized the network heat map in MRC5 (A) and A549 (B) cells under treatment of cytotoxic agents (Figure 6.). Our results also enhanced the metabolic differences between normal and cancer cells by identifying typical hub metabolites for each treatment group in MRC5 (A) and A549 (B) cells (Figure

7.). We determined lactate is the hub metabolites in 5-FU treated MRC5 cell group.

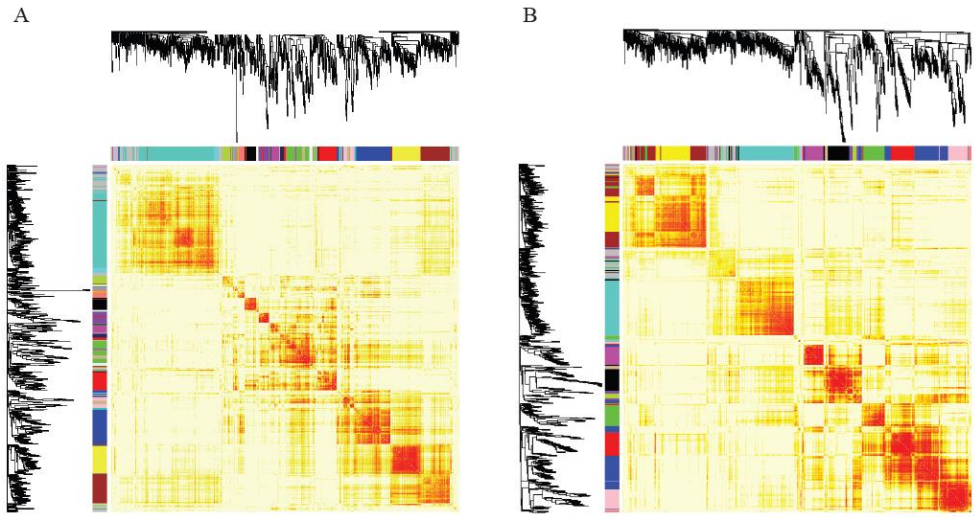

Figure 6. Weighted Correlation Network Analysis

Weighted correlation network analysis (WGCNA) of metabolic profiles of MRC5 (A) and A549 (B) cells under treatment of Cis-platin, Doxorubicin, and 5-FU.

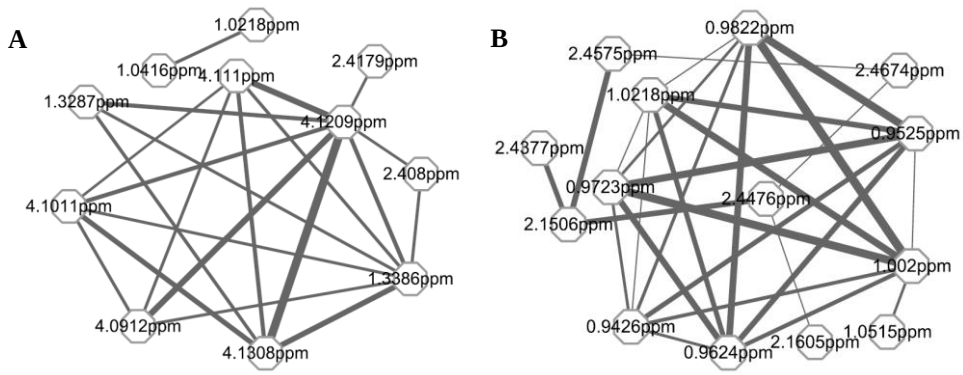

Figure 7. Hub Metabolites

Hub metabolites and their metabolic profile as represented by node and edge graph of MRC5 (A) and A549 (B) cell. The nodes connected with more edges were selected for the hub metabolite.

In A549 cells, isoleucine, leucine, valine, and glutamine were identified as hub metabolites for Cis-platin treated group, and glucose and phosphocholine were recognized as hub metabolites for 5-FU treated group (Table 2). WGCNA result showed that metabolites related to Warburg effect and reductive lipogenesis have high connectivity, and branched amino acids and phosphocholine are important in metabolic network. Comparing WGCNA with multivariate analysis, significant metabolites that had been identified in multivariate analysis were also determined as a hub metabolite in WGCNA, and therefore both analysis tools reached the common result. We found that metabolite alterations are different according to cellular metabolic states in response to cytotoxic agents, and metabolites related to Warburg effect and reductive lipogenesis are more important for cell survival than others.

Table 2. Hub Metabolites

	MRC5		A549	
	ppm	Hub metabolites	ppm	Hub metabolites
Cis-platin			1.0218, 1.002, 0.9822, 0.9723, 0.9624, 0.9525, 0.9426, 2.1506	Glutamine Isoleucine Leucine Valine
Doxorubicin				
5-FU	4.1308, 4.1209, 4.1011, 1.3386	Lactate	3.8536, 3.8437, 3.8239, 3.6754, 3.6655, 3.6556, 3.6457, 3.6358, 3.2199, 4.0417	Glucose Phosphocholine

Ⅳ. Discussion

While the target of cytotoxic agents has been characterized, the effects of these compounds on the cell metabolism, especially cancer cell metabolism, have not been fully understood. In cancer, some metabolites have been linked to cancer induction and treatment. Recently, many studies have highlighted the potential roles of single metabolites in cancer evolution and cancer diagnosis (7-10). The knowledge of cancer metabolism would enhance the effectiveness in cancer treatment. Specifically, how differently changed of metabolism in normal and cancer cell lines in response to cytotoxic agents would give valuable information for chemotherapy application in the clinical practice. Therefore, in this study, we have investigated metabolic alterations in response to cytotoxic agents in normal and cancer cell lines by 1H-NMR spectroscopy.

Results from MTT assay and NMR spectroscopy equally showed that metabolic alterations of A549 cancer cell groups were more noticeable than those of MRC5 normal cell groups in response to cytotoxic agents, and changes in 5-FU treated A549 cells were the most distinctive in all groups. Therefore, we supposed that metabolic alterations in each group are closely connected to the cell viability. Furthermore, PLS-DA data showed that cytotoxic agents influenced on the metabolic profiles of both MRC5 and A549 cells, not only A549 cells, and the

effect of cytotoxic agents was greatest in 5-FU treated A549 cells. Since metabolic profiles of MRC5 and A549 were both changed, we supposed that changing patterns of single metabolites could be important on the cell viability. The changes of individual metabolites were totally different between MRC5 and A549 cells after treating cytotoxic agents, as shown in heat map data.

Among these altered metabolites, glucose is a key carbon source to produce ATP and to synthesize biomass, and a starting material of glycolysis related to Warburg effect. Warburg effect is well known phenomenon in cancer metabolism, and has been targeted for cancer therapy (29). In response to cytotoxic agents, glucose in MRC5 cell was increased, but that in A549 was relatively constant, except slightly increased in 5-FU treated A549 cell group. First, in A549 cancer cell groups, although glucose level maintained stably, lactate was significantly increased. Since lactate is the final product in glycolysis pathway, it could be explained that the glycolysis pathway in cancer cells still works well. However, it is noted that in 5-FU treated A549 cell group, the increase of lactate was a little bit less and the increase of glucose was more than other treated groups of A549 cells. This result showed a relative reduction of glycolysis in 5-FU treated A549 cell group comparing to other agent-treated groups, which may be a worse condition for survival in cancer cells. Combining to the MTT assay results, such relative decrease in glycolysis is possibly explained to the increased cell death in 5-FU treated A549 cell group. This observation is suitable with previous study confirmed that combining chemotherapy with compounds that inhibit glucose uptake or initial

steps of glycolysis enhance cytotoxic effects of drugs in cancer cells (30). To the best of our knowledge, studies related to glucose uptake and catabolism in normal cells in response to cytotoxic agents have not been performed yet. However, we observed that glucose was increased in three MRC5 cell groups in response to cytotoxic agents, which is contrary to decreasing of other energy sources such as glutamine and other essential amino acids.

Glutamine is another carbon source for fueling cell metabolism through and is highlighted due to glutaminolysis and reductive lipogenesis pathway. That glutamine was increased in response to cytotoxic agents is consistent to previous several studies (31, 32). Glutaminolysis is induced by HIF-1 or MYC, which often up-regulated in cancer cell lines (15, 33). After treating cytotoxic agents, glutamine greatly increased in all three treated groups in A549 cells, but decreased in all three treated groups in MRC5. In A549 cells, not only glutamine, glutaminolysis intermediates such as glutamate and citrate were also increased in A549 cells. The fact that starting material, glutamine and glutaminolysis intermidates were all increased could be interpreted as glutaminolysis became slow or slightly blocked somewhere at the last stage. The metabolic changes of glutaminolysis in response to cytotoxic agents were not fully studied yet. However, as glutaminolysis has become an important target for cancer therapy, many attempts to block glutaminolysis, like using glutaminase inhibitors, have been made (34). We suggest that the decrease of glutaminolysis could connect with general decrease of cell viabilities in all treated groups of A549 cells.

Other altered metabolites are glutathione and taurine that are related to redox state (35, 36). In this study, glutathione was decreased in all treated groups of MRC5 cells, but increased in all A549 cells. It has been reported that glutathione is a ROS reducing metabolite. As shown in many studies, ROS can cause cell death or cellular damage (36). However, in this study, glutathione was increased in A549 cell groups where cell viability significantly decreased, and decreased in MRC5 cell groups where that remained unchanged. According to previous studies, glutathione showed a variation in concentration (2, 31). We suggest that oxidative stress will not be the direct cause of cell death in A549 cell groups due to the high glutathione in all the A549 cell groups. Other studies also showed that there was not a clear relationship between ROS and cell death for the cancer cells (2, 17). On the other hand, ROS might effect on the cell viability of MRC5 cell groups. Although cell viability did not decrease significantly ($p>0.05$), cell death of MRC5 slightly increased in Cis-platin treated and 5-FU treated groups where less glutathione was observed. The use antioxidant combining to chemotherapy in cancer is a still controversial issue, but it has been recommended on the toxicity decrease of chemotherapy (37, 38). Since glutamine restores the level of glutathione reduced by chemotherapy, glutamine supplement was also used to reduce the chemotherapy-induced toxicity (39, 40).

Branched amino acids, isoleucine, leucine, and valine showed the noticeable differences in response to cytotoxic agents between MRC5 and A549 cells. Branched amino acids are increased in all A549 cell groups, but decreased in all

MRC5 cell groups. Recent studies have demonstrated that branched amino acids promote metabolic diseases, and have connection with lipid (41, 42). Since branched amino acids, which are used to produce lipid, was increased in A549 cell groups, we anticipated that there is a problem on the lipid synthesis pathway. This also can be related to the decrease of reductive lipogenesis. Besides, branched amino acids produce glutamine on the first step of branched amino acids catabolism, and glutamate transfers the amino group from pyruvate to alanine (41). In this study branched amino acids, glutamine, glutamate, and alanine were all increased in A549 cell groups, showing the inter-correlation between metabolites.

Glycine also showed the different metabolic alterations between normal and cancer cells. Glycine increased in A549 cell groups and decreased in MRC5 cell groups in response to cytotoxic agents. Recent studies showed that the glycine was highly connected with the cell proliferation and increased glycine consumption appeared in rapidly proliferating cells (10). As glycine increased in A549 cell groups, it is supposed that glycine was not consumed for the rapid cell proliferation. The impairment in A549 cell proliferation is consistent with the decrease of cell viability in A549 cells shown in MTT assay data. Another study founded that increased glycine concentration impaired cell growth reducing the methylene-THF production for purine biosynthesis (43). Highly increased glycine concentration in A549 cell groups in response to all cytotoxic agents may be a harmful condition for cell growth.

We started this study from determining the concentration of cytotoxic agents in

which we observed the opposite changes of many metabolites between MRC5 and A549 cells. While MRC5 cells showed the general metabolic deficiency, A549 cells showed general metabolic enhancement. We interpreted the metabolic enhancement of A549 cells as a poor flow of various cellular pathways, because cancer cell viability decreased and cell proliferation was impaired. We determined the glutamine, glutamate, branched amino acid and glycine as biomarkers to predict the cancer cell death in response to cytotoxic agents. These metabolites were all highly increased in treated A549 cell groups and appeared the impairment of major metabolic pathways. In addition, we also identified glucose as specific biomarker that shows the severe cell death of cancer cells. 5-FU treated A549 cell group was characterized by not only an increased glutamine, but also an increased glucose level compared to the other treated A549 cell groups, which was accompanied by noticeable decrease of cell viability. Glutamine and glucose are main sources for ATP production and biomass biosynthesis. If glycolysis and glutaminolysis are both impaired, that will make cancer cells severely vulnerable. Recent study revealed that metabolic compensation occurred in glucose and glutamine utilization and simultaneous suppression should be made for blockage of cancer growth (44). Consequentially, multivariate data showed that metabolism of glucose and glutamine has a pivotal role for cancer cell survival.

In WGCNA, lactate was determined as hub metabolite for 5-FU treated MRC5 cell group. Glutamine and branched amino acids are recognized as hub metabolites for Cis-platin treated A549 cell group, and glucose and phosphocholine are

recognized for 5-FU treated A549 cell group. Since WGCNA also selected the metabolites related to glycolysis and glutaminolysis, same metabolites were identified in two methodologically different methods: multivariate analysis and WGCNA. We can analyze the individual metabolites by multivariate analysis and assess those metabolites in the connection with other metabolites by WGCNA. From two results, we concluded that two methodologically different analysis tools have their own advantageous and complementary property.

Taken together, the metabolic response in cancer cells is different from that in normal cells when treating with cytotoxic agents. Our metabolomics approach contributed to new knowledge to understand the mechanism behind the effect of cytotoxic drugs on both cancer and normal cells, which will help to provide adequate use of these drugs.

V. References

1. Hammel P, Hentic O, Neuzillet C, Faivre S, Raymond E, Ruszniewski P. New treatment options with cytotoxic agents in neuroendocrine tumours. Targeted oncology. 2012;7(3):169-72.

2. Duarte IF, Ladeirinha AF, Lamego I, Gil AM, Carvalho L, Carreira IM, et al. Potential markers of cisplatin treatment response unveiled by NMR metabolomics of human lung cells. Molecular pharmaceutics. 2013;10(11):4242-51.

3. Ham MS, Lee JK, Kim KC. S-adenosyl methionine specifically protects the anticancer effect of 5-FU via DNMTs expression in human A549 lung cancer cells. Molecular and clinical oncology. 2013;1(2):373-8.

4. Lv S, Tang Z, Li M, Lin J, Song W, Liu H, et al. Co-delivery of doxorubicin and paclitaxel by PEG-polypeptide nanovehicle for the treatment of non-small cell lung cancer. Biomaterials. 2014;35(23):6118-29.

5. Siddik ZH. Cisplatin: mode of cytotoxic action and molecular basis of resistance. Oncogene. 2003;22(47):7265-79.

6. Schulze A, Harris AL. How cancer metabolism is tuned for proliferation and vulnerable to disruption. Nature. 2012;491(7424):364-73.

7. Possemato R, Marks KM, Shaul YD, Pacold ME, Kim D, Birsoy K, et al. Functional genomics reveal that the serine synthesis pathway is essential in breast cancer. Nature. 2011;476(7360):346-50.

8. Metallo CM, Gameiro PA, Bell EL, Mattaini KR, Yang J, Hiller K, et al. Reductive glutamine metabolism by IDH1 mediates lipogenesis under hypoxia. Nature. 2012;481(7381):380-4.

9. Lee AS. Glucose-regulated proteins in cancer: molecular mechanisms and therapeutic potential. Nature reviews Cancer. 2014;14(4):263-76.

10. Jain M, Nilsson R, Sharma S, Madhusudhan N, Kitami T, Souza AL, et al. Metabolite profiling identifies a key role for glycine in rapid cancer cell proliferation. Science. 2012;336(6084):1040-4.

11. Vander Heiden MG, Cantley LC, Thompson CB. Understanding the Warburg effect: the metabolic requirements of cell proliferation. Science. 2009;324(5930):1029-33.

12. Akakura S, Ostrakhovitch E, Sanokawa-Akakura R, Tabibzadeh S. Cancer cells recovering from damage exhibit mitochondrial restructuring and increased aerobic glycolysis. Biochemical and biophysical research communications. 2014.

13. Phan LM, Yeung SC, Lee MH. Cancer metabolic reprogramming: importance, main features, and potentials for precise targeted anti-cancer therapies. Cancer biology & medicine. 2014;11(1):1-19.

14. DeBerardinis RJ, Mancuso A, Daikhin E, Nissim I, Yudkoff M, Wehrli S, et al. Beyond aerobic glycolysis: transformed cells can engage in glutamine metabolism that exceeds the requirement for protein and nucleotide synthesis. Proceedings of the National Academy of Sciences of the United States of America. 2007;104(49):19345-50.

15. Wise DR, DeBerardinis RJ, Mancuso A, Sayed N, Zhang XY, Pfeiffer HK, et al. Myc regulates a transcriptional program that stimulates mitochondrial glutaminolysis and leads to glutamine addiction. Proceedings of the National Academy of Sciences of the United States of America. 2008;105(48):18782-7.

16. Benjamin DI, Cozzo A, Ji X, Roberts LS, Louie SM, Mulvihill MM, et al. Ether lipid generating enzyme AGPS alters the balance of structural and signaling lipids to fuel cancer pathogenicity. Proceedings of the National Academy of Sciences of the United States of America. 2013;110(37):14912-7.

17. Zhu C, Hu W, Wu H, Hu X. No evident dose-response relationship between cellular ROS level and its cytotoxicity - a paradoxical issue in ROS-based cancer therapy. Scientific reports. 2014;4:5029.

18. Tripathi P, Somashekar BS, Ponnusamy M, Gursky A, Dailey S, Kunju P, et al. HR-MAS NMR tissue metabolomic signatures cross-validated by mass spectrometry distinguish bladder cancer from benign disease. Journal of proteome research. 2013;12(7):3519-28.

19. Irfan A, Cauchi M, Edmands W, Gooderham NJ, Njuguna J, Zhu H. Assessment of temporal dose-toxicity relationship of fumed silica nanoparticle in human lung A549 cells by conventional cytotoxicity and (1)H-NMR-based extracellular metabonomic assays. Toxicological sciences : an official journal of the Society of Toxicology. 2014;138(2):354-64.

20. Akira K, Hichiya H, Morita M, Shimizu A, Mitome H. Metabonomic study on the biochemical response of spontaneously hypertensive rats to chronic

taurine supplementation using (1)H NMR spectroscopic urinalysis. Journal of pharmaceutical and biomedical analysis. 2013;85:155-61.

21. Kim J, Keay SK, Dimitrakov JD, Freeman MR. p53 mediates interstitial cystitis antiproliferative factor (APF)-induced growth inhibition of human urothelial cells. FEBS letters. 2007;581(20):3795-9.

22. Chaneton B, Hillmann P, Zheng L, Martin AC, Maddocks OD, Chokkathukalam A, et al. Serine is a natural ligand and allosteric activator of pyruvate kinase M2. Nature. 2012;491(7424):458-62.

23. Kang J, Lee S, Kang S, Kwon HN, Park JH, Kwon SW, et al. NMR-based metabolomics approach for the differentiation of ginseng (Panax ginseng) roots from different origins. Archives of pharmacal research. 2008;31(3):330-6.

24. Wen H, Kang S, Song Y, Song Y, Sung SH, Park S. Differentiation of cultivation sources of Ganoderma lucidum by NMR-based metabolomics approach. Phytochemical analysis : PCA. 2010;21(1):73-9.

25. Kang J, Choi MY, Kang S, Kwon HN, Wen H, Lee CH, et al. Application of a 1H nuclear magnetic resonance (NMR) metabolomics approach combined with orthogonal projections to latent structure-discriminant analysis as an efficient tool for discriminating between Korean and Chinese herbal medicines. Journal of agricultural and food chemistry. 2008;56(24):11589-95.

26. Wen H, Yoo SS, Kang J, Kim HG, Park JS, Jeong S, et al. A new NMR-based metabolomics approach for the diagnosis of biliary tract cancer. Journal of hepatology. 2010;52(2):228-33.

27. Langfelder P, Horvath S. WGCNA: an R package for weighted correlation network analysis. BMC bioinformatics. 2008;9:559.

28. Wang J, Chen L, Tian X, Gao L, Niu X, Shi M, et al. Global metabolomic and network analysis of Escherichia coli Responses to exogenous biofuels. Journal of proteome research. 2013;12(11):5302-12.

29. Elf SE, Chen J. Targeting glucose metabolism in patients with cancer. Cancer. 2014;120(6):774-80.

30. Simons AL, Ahmad IM, Mattson DM, Dornfeld KJ, Spitz DR. 2-Deoxy-D-glucose combined with cisplatin enhances cytotoxicity via metabolic oxidative stress in human head and neck cancer cells. Cancer research. 2007;67(7):3364-70.

31. Liu S, Wang W, Zhou X, Gu R, Ding Z. Dose responsive effects of cisplatin in L02 cells using NMR-based metabolomics. Environmental toxicology and pharmacology. 2014;37(1):150-7.

32. Lodi A, Ronen SM. Magnetic resonance spectroscopy detectable metabolomic fingerprint of response to antineoplastic treatment. PloS one. 2011;6(10):e26155.

33. Dewhirst MW, Cao Y, Li CY, Moeller B. Exploring the role of HIF-1 in early angiogenesis and response to radiotherapy. Radiotherapy and oncology : journal of the European Society for Therapeutic Radiology and Oncology. 2007;83(3):249-55.

34. Zhao Y, Butler EB, Tan M. Targeting cellular metabolism to improve cancer therapeutics. Cell death & disease. 2013;4:e532.

35. Jang HJ, Kim SJ. Taurine exerts anti-osteoclastogenesis activity via inhibiting ROS generation, JNK phosphorylation and COX-2 expression in RAW264.7 cells. Journal of receptor and signal transduction research. 2013;33(6):387-91.

36. Gorrini C, Harris IS, Mak TW. Modulation of oxidative stress as an anticancer strategy. Nature reviews Drug discovery. 2013;12(12):931-47.

37. Vincent DT, Ibrahim YF, Espey MG, Suzuki YJ. The role of antioxidants in the era of cardiooncology. Cancer chemotherapy and pharmacology. 2013;72(6):1157-68.

38. Crawford S. Anti-inflammatory/antioxidant use in long-term maintenance cancer therapy: a new therapeutic approach to disease progression and recurrence. Ther Adv Med Oncol. 2014;6(2):52-68.

39. Gaurav K, Goel RK, Shukla M, Pandey M. Glutamine: A novel approach to chemotherapy-induced toxicity. Indian journal of medical and paediatric oncology : official journal of Indian Society of Medical & Paediatric Oncology. 2012;33(1):13-20.

40. Braga-Neto MB, Warren CA, Oria RB, Monteiro MS, Maciel AA, Brito GA, et al. Alanyl-glutamine and glutamine supplementation improves 5-fluorouracil-induced intestinal epithelium damage in vitro. Digestive diseases and sciences. 2008;53(10):2687-96.

41. Newgard CB. Interplay between lipids and branched-chain amino acids in development of insulin resistance. Cell metabolism. 2012;15(5):606-14.

42. Cha JH, Bae SH, Kim HL, Park NR, Choi ES, Jung ES, et al. Branched-chain amino acids ameliorate fibrosis and suppress tumor growth in a rat model of hepatocellular carcinoma with liver cirrhosis. PloS one. 2013;8(11):e77899.

43. Fan J, Ye J, Kamphorst JJ, Shlomi T, Thompson CB, Rabinowitz JD. Quantitative flux analysis reveals folate-dependent NADPH production. Nature. 2014;510(7504):298-302.

44. Lim JH, Luo C, Vazquez F, Puigserver P. Targeting Mitochondrial Oxidative Metabolism in Melanoma Causes Metabolic Compensation through Glucose and Glutamine Utilization. Cancer research. 2014;74(13):3535-45.

국문초록

Cytotoxic agents 를 처리하였을 때 정상세포와 암세포에서 metabolic profile 의 비교

이 수 진

서울대학교 약학대학원

약학과 천연물과학전공

방사선 치료와 더불어, cytotoxic agents 를 사용하는 화학 요법은 cancer 치료에 가장 널리 사용되는 치료법 중의 하나이다. cytotoxic agents 는 cell 의 DNA 에 damage 를 주어 cell survival 을 감소시키는데, 그 과정에서 대사의 변화는 아직 명확히 알려져 있지 않다. 우리는 여기에서 폐 정상 세포인 MRC5 cell 과 폐 암 세포인 A549 cell 에 폐암에 일반적으로 사용되는 cytotoxic agents 인 Cis-platin, Doxorubicin, 그리고 5-Fluorouracil (5-FU)를 처리하여 cell viability 를 확인하였다. cell viability 는 3 일 동안 agents 를 처리한 후에 확인하였으며, MTT assay 로 평가하였다. agents 의 농도는 Cis-platin, Doxorubicin, 그리고 5-FU 에서 각각 0.813 mg/ml, 0.13

mg/ml, and 0.0332 mg/ml 이었고, 이 농도에서 A549 의 viability 는 유의성 있게 감소한 반면 (p-value=0.001), MRC5 의 viability 는 유의성 있는 변화를 보이지 않았다 (p-value=0.358). 이러한 세포 viability 차이와 연관된 cell metabolism 의 변화를 알아보고자 metabolic profile 의 변화를 1H-NMR spectrometry 를 사용하여 확인하였다. NMR data 에서 agents 를 처리한 후 A549 cell 의 metabolic profile 이 MRC5 cell 에 비해 더 많이 변화하였고, A549 cell 에 5-FU 를 처리하였을 때 처리한 agents 중에서 가장 뚜렷한 차이를 보였다. Heat map analysis 를 하였을 때 두 그룹의 metabolite 의 변화는 확연한 차이를 보였다. Multivariate analysis 와 Weighted correlation network analysis (WGCNA)를 통해 두 그룹 간에 유의성 있게 차이를 보인 metabolites 와 hub metabolites 를 확인하였다. 서로 상반된 두 방법으로 분석을 하였을 때 cytotoxic agents 에 따라 달라진 metabolites 는 Warburg effect 그리고 Reductive lipogenesis 와 높은 상관관계를 가지고 있었고, 그 두 pathway 가 cell survival 에 중요한 영향을 미치는 것으로 여겨졌다. 요약하면, 우리는 normal cell 과 cancer cell 에 cytotoxic agents 를 처리하였을 때 cell viability 의 차이를 metabolomics 의 관점에서 확인하였다.

주요어: 폐암세포, 항암제, 세포독성, 대사 프로파일, 핵자기공명분광법

학번: 2012-23595